Sensors and Decoding for Intracortical Brain Computer Interfaces

Mark L. Homer,[1] Arto V. Nurmikko,[2] John P. Donoghue,[4,3] and Leigh R. Hochberg[4,2,5]

[1]Biomedical Engineering, [2]School of Engineering, [3]Department of Neuroscience, Brown University, Providence, Rhode Island 02912; email: Leigh_Hochberg@brown.edu

[4]Center for Neurorestoration and Neurotechnology, Veterans Affairs Medical Center, Providence, Rhode Island 02908

[5]Neurology, Massachusetts General Hospital, Harvard Medical School, Boston, Massachusetts 02114

Annu. Rev. Biomed. Eng. 2013. 15:383–405

The *Annual Review of Biomedical Engineering* is online at bioeng.annualreviews.org

This article's doi:
10.1146/annurev-bioeng-071910-124640

Keywords

brain machine interfaces, multielectrode arrays, signal processing, neural engineering

Abstract

Intracortical brain computer interfaces (iBCIs) are being developed to enable people to drive an output device, such as a computer cursor, directly from their neural activity. One goal of the technology is to help people with severe paralysis or limb loss. Key elements of an iBCI are the implanted sensor that records the neural signals and the software that decodes the user's intended movement from those signals. Here, we focus on recent advances in these two areas, placing special attention on contributions that are or may soon be adopted by the iBCI research community. We discuss how these innovations increase the technology's capability, accuracy, and longevity, all important steps that are expanding the range of possible future clinical applications.

Contents

INTRODUCTION

Voluntary limb movement in primates, including able-bodied people, is achieved in part by the conveyance of high-level motor commands from neurons in the motor cortex to neurons within the spinal cord. In response to input from these so-called upper motor neurons, as well as inputs from other descending systems and cells local to the spinal cord, alpha (lower) motor neurons then activate muscle fibers to generate motion. Injury or disease, such as brain stem stroke or loss of a limb, can disconnect the cortex from its effector target. Ongoing research is focused on building technological bridges between the motor cortex and external devices in order to restore motor function. When these systems work as designed, the intent to move again becomes translated into overt action.

Variously labeled as neural interfaces, neural prostheses, brain machine interfaces (BMIs), or brain computer interfaces (BCIs), this technology promises to be useful to a large number of people. In the United States alone, it is estimated that 1.6 million Americans live with limb loss (1), and 5.5 million people experience some form of paralysis (2), including 50,000 individuals who have complete tetraplegia (severe functional impairment or paralysis of both arms and legs) (3). Commonly, people with tetraplegia rely on others to perform routine, everyday actions. Responding to the need for better assistive devices, BCI technology could provide a control signal for any range of devices, from a computer to robotic or prosthetic arms to a powered wheelchair. For a true restoration of function, people with arm paralysis might, in the future, be able to recover control by reanimating the affected muscles via brain-controlled functional electrical stimulation (FES); others with limb loss could employ a robotic prosthesis that emulates arm and hand actions.

This review focuses on intracortical brain computer interfaces (iBCIs) in which, for example, microscale probes having 96 fine-tipped microelectrodes in a compact 4 $\times$ 4–mm array are inserted into the cortex (reviews of scalp-based electroencephalography and brain surface–based electrocorticography BCIs can be found in References 4 and 5, respectively). The sensors are sensitive enough to pick up the discrete output of single neurons; the action potential, commonly referred to as a spike; and the summed voltage fluctuations from small to large numbers of neurons, which are called field potentials. Each electrode provides spiking from up to a few neurons (typically one or two), yielding the population's time-evolving output pattern. These represent but a small sample of the entire set of neurons in this limited region, as spiking can be detected only by microelectrodes closely approximated to a neuron.

Spikes are useful because they are the information-rich signal nearly universally employed by neurons for communication in the nervous system. Beginning approximately 50 years ago, experiments by Evarts and others revealed how individual cortical neurons, recorded one at a

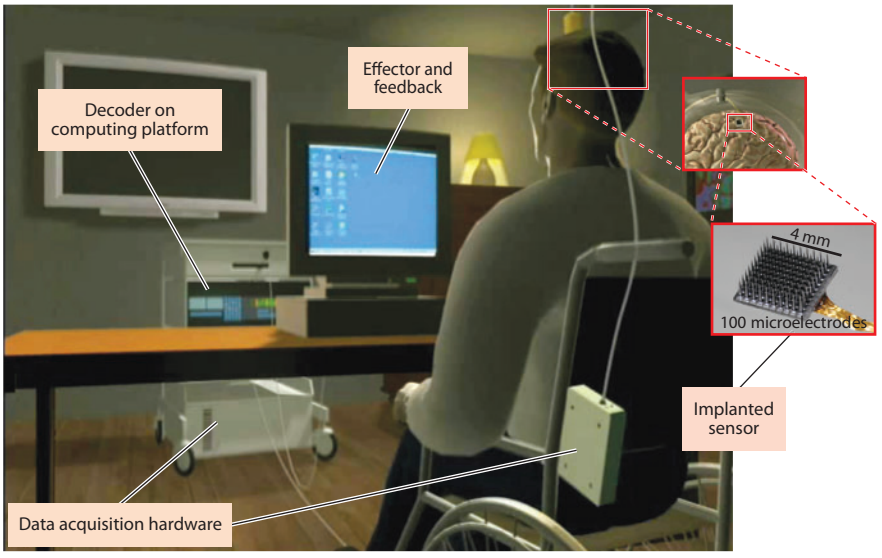

Figure 1

Illustration of an iBCI setup.

time, control voluntary movement, helping to lay the groundwork for current iBCI research (see e.g., 6–11). Multielectrode approaches (12, 13) provided early examples of real-time prediction of an animal's wrist position from the decoded motor cortex output (14, 15) and enabled animals to perform simple tasks via an external device (16). The first clinical realization of these technologies occurred in 1998, when a person with amyotrophic lateral sclerosis (ALS) paralysis controlled an on-off switch using two electrodes implanted in the motor cortex (17).

Based upon many years of publicly funded basic science, research beginning in 2000 demonstrated that monkeys could use motor cortex spiking patterns to control a computer cursor in two or three dimensions (18–22). Soon afterward, in 2004, the first demonstrations of intracortically directed two-dimensional (2D) cursor movements and simple robotic control were accomplished by people with tetraplegia using an iBCI (23). This was followed by iBCI-enabled three-dimensional (3D) control of a prosthetic arm by nonhuman primates (24). Most recently, multidimensional robotic arm control was successfully achieved for reaching and grasping actions by people with tetraplegia (25, 26). The future promise of brain-controlled FES devices was also demonstrated through iBCI-driven muscle control in monkeys with temporary arm paralysis (27–29), an achievement that further underscored the potential highlighted in an initial demonstration by a human with paralysis using an iBCI to control a simulated, dynamic FES system and arm (30).

Modern iBCIs have several major components, as illustrated in **Figure 1**. The user imagines or attempts a movement, resulting in motor cortical neuronal activity. An implanted multiprobe sensor of electrodes, commonly referred to as a microelectrode array (MEA), records neural activity in the form of extracellular voltage signals. Data acquisition (DAQ) hardware transports, amplifies, and digitally samples these signals. The data are processed on a dedicated, real-time hardware and software platform, which hosts various decoding routines. In the typical real-time data processing stream, first neural signals are processed to extract informative features related to intended movement, and then estimation techniques translate those features into device commands. The entire decoding procedure typically executes in under 100 ms. The device then carries out the desired action and provides feedback to the user.

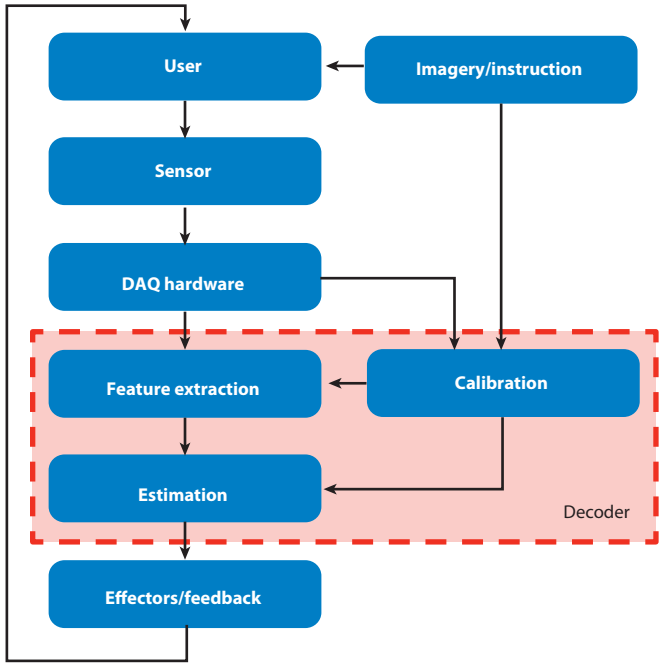

Figure 2

Block diagram of iBCI architecture. Arrows indicate the major flows of information, and the red-shaded box contains elements associated with decoding.

The core elements of an iBCI (**Figure 2**), from neural signal collection to actuation of the effector, each require the iBCI neuroengineering team to make important decisions. Each of these elements (which could also be broken into several smaller elements) also presents opportunities for focused research and development. In this review, we take the engineering perspective, which sees the domain of decoding as encompassing the combination of the feature extraction, estimation, and calibration elements (31); this viewpoint is used to organize subsequent sections.

Prior to use, the iBCI must be calibrated. Plainly stated, a map must be built between the observed neural activity associated with intended movement and the actual movement of the effector. First, the user (with, for example, tetraplegia due to stroke or ALS) engages in a series of instructed behavioral tasks in which various real world actions, such as the preprogrammed motion of a computer cursor, are observed while imagined or attempted by the user (who is unable to perform them). Next, with both the neural signals and the attempted (or, at least, instructed) movements being known quantities, calibration techniques tune the decoder. It is important to note that during this process only the decoder has been calibrated; no real training or learning has (yet) occurred from the user's standpoint. Although it is reasonable to believe that users presented with a new and reasonably useful tool (an iBCI) will become more proficient in its use over time (32), important questions regarding recorded signal stability as well as the potential for simultaneous coadaptation (33) of both the decoder and the user leave the clear demonstration of such learning to future research.

A thorough review of the several active research areas highlighted in **Figure 2** would extend far beyond this review (see Reference 34 for several excellent chapters in this regard). Here we focus on recent advances using the implanted sensor as well as the state of the art in decoding

algorithms. In each case, the emphasis is on results that have been or that we believe are likely to be widely adopted by the iBCI research community.

IMPLANT

Microelectrode Arrays

Overview. From an electrical and electrophysiological point of view, MEAs for iBCIs need to be designed considering details of both the electrode-brain tissue interface and the macroscale (i.e., lumped) circuit equivalents. Quantitative modeling for optimizing capture of the neuronal electrical signals is complex, influenced by the role of the electrolytic bilayer at the interface between the electrode recording surface and brain tissue, electrode tip shapes, potential tissue reactions, etc. (35). Metals such as Pt, W, and Ir are chemically stable in the electrolyte-rich and proteinaceous environment of brain parenchyma and have reasonable work functions to match the Na^+, K^+, Cl^-, Ca^{2+}, and Mg^{2+} concentrations that dominate. To capture both spikes and lower-frequency field potentials, the equivalent circuit of the single microelectrode/tissue recording interface should typically cover a bandwidth of ~0.5 Hz–10 kHz. A single action potential might generate recorded amplitudes from a few tens up to more than a hundred microvolts, registered by an electrode of ~500-kΩ impedance (i.e., subnA currents), thereby framing the design requirements for subsequent analog preamplifiers (gain, noise figure, etc.), digitizing circuits, and downstream signal processing and data management electronics. Note that apart from fundamental sources of noise common to all electrical systems (Johnson noise, etc.), the brain operates within its own inherently noisy background (because its circuits are continuously alive), thereby adding to the challenges of MEAs acquiring consistent neural signals that correlate with a specific cognitive process or behavior. Another set of important contemporary questions relate to how reaction by the biologic tissue on implantable electrodes and related device structures affects their truly long-term chronic performance ($\gg$1 year).

Early intracortical MEAs composed of bundles of wires have now been largely replaced by monolithic arrays for work in primates. Of these, we mention the Si-based arrays in which lithographic and electrochemical techniques are combined to fabricate tapered, microscale beds of electrodes (36–38). For example, in the so-called Utah MEA (**Figure 3**, *inset*), each approximately conically shaped 1–1.5-mm-long electrode, with its p-Si shank insulated by biocompatible parylene, is coated at its tip with Pt or Pt/Ir. The heavily doped p-Si provides a low-loss conducting path onto the Si-insulated, planar support substrate from which a wire-bonded bundle (containing 100 insulated 1-mil Au wires) transports the recorded neural signals across the skull to a percutaneous connector that permits access to exterior electronics (**Figure 3**). Operationally, specialized neurosurgical techniques are employed to access cortical areas of interest, identify recording sites, and ultimately insert the MEAs. For the example of a 4 × 4–mm array with 100 electrodes of 1–1.5-mm length at a 400-μm pitch, techniques (including either frame-requiring or frameless stereotactic navigation) allow identification of the location on the skull under which lies the so-called knob (39) of the precentral gyrus. This well-documented anatomic landmark can identify the putative arm-hand area of the motor cortex. With the site located, surgeons can insert the MEA using instruments such as a pneumatic drive.

The presently employed procedure leads one to wonder whether the precise location of electrode array placement is important, or not, for deriving optimal iBCI-based control. Even with high resolution preoperative MR imaging, the presence of small surface vasculature and the presence of slight dimples in the cortical surface might lead to the decision to shift placement of the array by a few millimeters in any direction. Furthermore, although the gross cortical

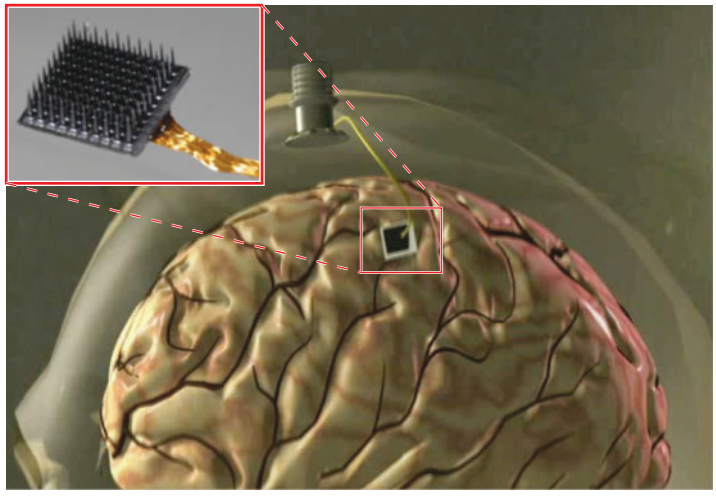

Figure 3

A silicon-based cortical microelectrode array (*inset*) implanted for intracortical neural recording via a percutaneous connection to a skull-mounted pedestal connector.

stimulation–based face-arm-leg somatotopy of motor cortex known since the late 1800s is undoubtedly correct, there is no such somatotopy at the resolution of single neurons recorded in a particular region of motor cortex. When we combine this underlying heterogeneity of neuronal function with the essentially random cohort of neurons from which signals are recorded, it would seem difficult to control for some important variables. Luckily, with the high redundancy of information in motor cortex at the level of single neurons, it seems likely that array-based intracortical recordings will consistently yield useful recordings. We and others have also begun to use functional magnetic resonance imaging (fMRI) to identify potentially useful locations for array placement. However, the relationship between the blood-oxygen-level-dependent (BOLD) signal for fMRI and the spiking activities of underlying neurons continues to be an evolving science; the use of fMRI may become more important as arrays begin to be placed in areas other than the precentral gyrus, where additional evidence of motor volition–related neural activity will be informative.

Although these MEA implants have shown their mettle as chronically viable implants as described in this review, further improvements in their reliability and further control of their critical dimensions on the micrometer scale are expected from improvements to current manufacturing approaches and from innovations in both materials and advanced microfabrication, such as, for example, wafer-scale processing (40).

Based on Si-substrate shanks, the Michigan array can run multiple connective lines down to pads of Ir along a shank to achieve multidepth electrodes (38). One shank can efficiently support as many as 16 electrode sites at different depths and can also horizontally cluster electrodes by placing several at the same depth along a single shank (41). Conducting polymer nanotubes have also been used to dramatically decrease impedance when attached to the surface of the electrode sites (42), potentially enabling the creation of thinner but still functional recording electrodes (43) that can be more densely placed in cortex without overly disturbing the surrounding tissue. Yet another technology, the neurotrophic electrode (17), aims to provide for long-term intracortical recordings by attracting the growth of neurites into a wire electrode–embedded glass enclosure.

Wireless implants. Several successful clinical technologies have benefitted from having percutaneous components during their initial development and testing (e.g., cardiac pacemakers, deep brain stimulators). Nevertheless, there are a number of aesthetic and safety benefits to developing systems that dispense with an externalized tether and that ultimately become fully implanted. One current research trend focuses on efforts to integrate the intracortical microelectrode recording arrays with wireless electronics so that the physical, cabled connection between a subject and external electronics and external assistive devices can be removed. Wireless approaches will greatly improve a subject's mobility, be that in human neuroprosthetic applications or in freely moving nonhuman primates in fundamental neuroscience research. Many groups worldwide are now working toward wireless active microelectronic neural interfaces, especially those focusing on very-low-power, system-on-chip application-specific integrated circuits (SoC/ASIC) that consolidate the analog, digital, and telemetric components to a wearable system. Several sophisticated designs have been demonstrated at the benchtop level. Yet, much of this integrated ASIC-based engineering work still awaits transition to in vivo use for primates. One successful strategy has been to retain the percutaneous wiring from the MEA to the skull-mounted connector pedestal and affix battery-powered, head-mounted external modules on these pedestals in nonhuman primates to demonstrate transmission of multichannel neuronal data as a broadband radiofrequency digital stream (44–47).

Transcutaneous systems. The emergent wireless approaches to iBCIs have the goal of eventual implementation as fully implanted electronic microsystems in which neural signals from MEAs are amplified and transmitted from hermetically sealed modules that are embedded entirely within the body (head, or head and chest), without any skin-penetrating wiring. The ability to employ fully wireless, and eventually bidirectional, iBCI interfaces that are enveloped by the body's most potent protection against infections, etc.—namely, the skin—potentially opens up entirely new vistas for next generations of neurotechnologies. As a state-of-the-art example from 2012, we show in **Figure 4*a*** a 100-channel, wireless neural broadband implant that has been successfully tested in mobile pig and nonhuman primate models (48, 49). The device shares a commonality with cochlear and cardiac implants in that the active microelectronics, battery power, and telemetry circuits are encased within a hermetically sealed Ti enclosure. In contrast to these low-data-rate neural stimulation devices, however, the amount of information that is being acquired wirelessly from the brain and transmitted through the skin to nearby receivers for decoding is huge (on the order of 50 Mbps at this writing and expected to increase in the future). Such demands on data rates not only impact the required sophistication in designing and fabricating the wireless implants but will require new strategies for handling and storing user-specific neural information in the future.

DECODING

Neural Signal Feature Extraction

Overview. Although recording with tens to more than 100 electrodes is common (18–26), the number of informative neural features required to control an iBCI can be much lower. Approximately 18 features were needed for monkeys to achieve 3D control in a virtual environment (19). More recently, people with tetraplegia successfully accomplished reach and grasp using a robotic arm with feature counts sometimes below 50 (25, 26). Although increasing the number of features can drive performance higher, a law of diminishing returns typically takes hold (50), at least when increasing the number of neurons recorded from a single cortical area. The challenge is less a

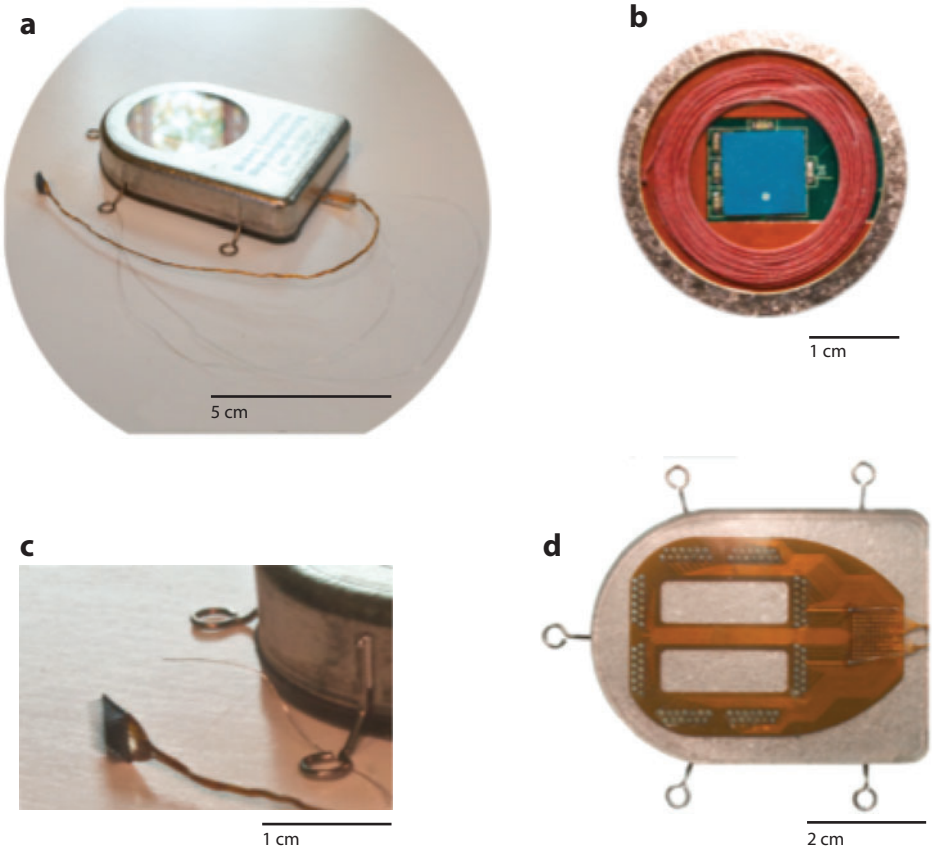

Figure 4

A wireless neural interface, hermetically sealed. (*a*) An image of the device after hermetic closure and ready for implant (device placed in special holder for sterilization and transport to the operating room). The standard 10 × 10–element microelectrode array (Blackrock Microsystems, UT) can be seen exiting the enclosure in a 100-wire bundle. (*b*) In a view through the single-crystal sapphire window, used for electromagnetic transparency, the receiving power coil (*red*) and the wideband data telemetry chip RF antenna (*blue*) can be seen. The sapphire is brazed to the Ti, maintaining the hermetic seal. (*c*) The intracortical neural sensor and a reference wire can be seen in relation to the epicranial/subcutaneous enclosure. (*d*) All 100 wires individually enter the enclosure through gold and ceramic feedthroughs, after being fanned out onto a flexible polymer (Kapton®) interconnect board sealed to the (outside) bottom of the Ti enclosure. Here, we show the 100-wire bonding site (grid, *right*) and the interconnect circuit board soldered to the feedthrough assembly. The interconnect board is packaged in biocompatible silicone rubber to maintain robust electrical isolation of the input electrodes.

matter of maximizing the number of electrodes with physiologically active signals than of recording signals each containing information highly relevant to motor control, but not redundant with the content in the other voltage channels.

The first decoding step is to extract information from the neural signals (**Figure 5**). During each operational cycle of the decoder (i.e., time step), a vector of values is computed from the multivariate time series sampled from the many voltage waveforms streaming in from the sensor. One classical approach depends upon the visual inspection of the action potentials (spikes) emanating from individual neurons (e.g., 23), in which spikes are a complex time derivative of the

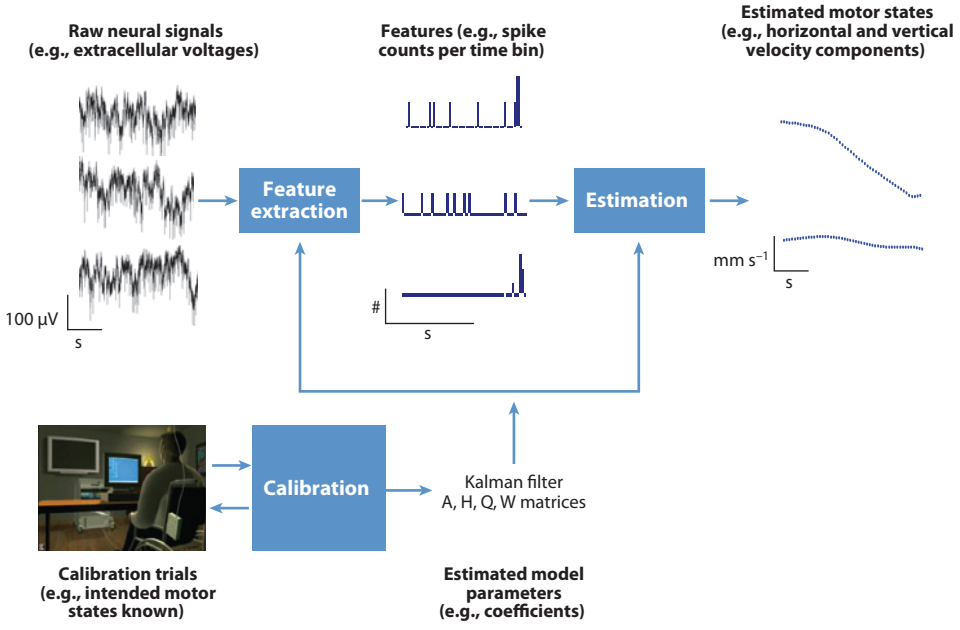

Figure 5

Illustration of a decoder's architecture and the flow of information passing through the various components. Matrices A, H, W, and Q represent model parameters in the Kalman filter. Specifically, A represents the motor state transition matrix, and W is the covariance matrix on the respective noise. Similarly, H captures how the neural features vary as a function of motor state (the observation matrix), and Q is the covariance matrix on the associated noise.

extracellular voltage gradients shaped by filter settings. The typically biphasic, millisecond-long voltage waveforms of each channel are visually inspected to manually set time and amplitude windows, converting them to discrete events in time, thus permitting detection of spikes and their assignment to a single neuron or a cluster of them. A unit's spikes are then time binned to compute the spike counts of each unit in each of the time bins, creating a point process time series for each channel.

Threshold crossings. Ideally, the recorded neurons and their associated features would remain stable for extended periods of time (i.e., decades). Over time, however, the statistical nature of the extracted features can change unexpectedly (e.g., 20, 49, 51, 52, 53). Eighty-four percent of the features exhibited such nonstationary behavior while people with tetraplegia operated an iBCI (54). The phenomenon occurred during blocks of trials spanning several minutes. In 15% of these instabilities, the combination of time-amplitude bins traditionally used in spike sorting failed to detect spikes, owing to drifts in their amplitude that result from even small movements (on the order of a few tens of micrometers of the electrode recording site with respect to a particular neuron). If left unmitigated, iBCI performance can degrade.

A simpler and more robust approach may be to count the number of voltage threshold crossings within a given channel and time bin (55). By detecting threshold crossings, the technique enabled no appreciable drop in decoding performance despite significant reductions in spike amplitudes (53). Use of threshold crossings is gaining adoption and has been a key element in recent pilot

clinical studies (25), but success may be sensitive to signal-to-noise ratio, electrode properties, the size and shape of neurons, and other unknown factors.

Multiunit activity. An alternative or addition to detecting spikes analyzes signal fluctuations available in the high-frequency band (i.e., 300–6,000 Hz). The multiunit activity (MUA) can also be used for iBCI control after passing through signal processing such as a nonlinear filter (56). More recently, in off-line decoding, nonlinear filtering of MUA was reported to yield better results than either spike detection and sorting or threshold crossing (57). Three-dimensional reach and grasp in monkeys was decoded off-line by extracting power information in the 200–400-Hz frequency band (which extends into the MUA range) (58). In preliminary closed-loop, head-to-head comparisons of a person with tetraplegia operating an iBCI, MUA performance was found comparable to that of spike counts (59). Perhaps most attractive is the evidence given of MUA's nonstationary statistics being less pronounced than other high-frequency signal options (57). Again, caution is needed because these advantages may be modified by amplifier or electrode properties.

Local field potentials. Other frequency bands within the range of signals generated by neural activity also contain information about movement intent. Unlike spikes, the primary sources for a given local field potential (LFP) measured in the motor cortex remain unclear. Although it has been postulated that LFPs are the result of synaptic currents, many factors such as spike afterhyperpolarizations can play a role (60). Prominent oscillations, one example of which is commonly referred to as beta rhythm, have been linked to attention (61) and found to noticeably decrease in amplitude between movement preparation and onset (11). In the past decade, reach direction was decoded from LFPs in monkeys in off-line studies (62–64). The feature extraction method varied from, for example, a Gaussian kernel smoother (62) to a multitaper spectral analysis (64). The frequency bands studied may contain different types of information about intended movement; for example, the average amplitude within the 63–200-Hz band increased at movement onset relative to baseline, whereas it was observed to decrease in the 16–42-Hz range (63). Three-dimensional reach and grasp in monkeys can be decoded, off-line, from intracortically recorded low, midrange, and higher frequency bands, with quality approaching, but not surpassing, that of spikes (65). **Figure 6** provides an example recorded from a person with tetraplegia with a sensor placed in the arm area of motor cortex. In the presented spectrogram, there is a decrease in amplitude during intended arm movement in the 12–40-Hz range, with both increases and decreases in power seen at other frequency bands throughout the intended movement.

Using two arrays and frequency bands, 0.3–4 Hz and 48–200 Hz, classification of eight target directions was achieved to an accuracy comparable to that of spikes (66). Other reports decoded natural arm reaches to predict arm end-point motion and grip aperture (65, 67). Despite these advances, comparisons between decoding with LFPs versus spikes do not point to LFPs as a clear winner (62, 65). The real value then of the signal is thought to lie in providing more robust features, particularly over the course of time. For example, the ability to detect a spike might be susceptible to array micromotions, whereas the aggregate nature of LFPs may mitigate signal changes due to tiny array movements because of their volume conduction properties. This advantage might explain one study's report of channels that had lost their spikes still retaining most of their predictive power in the LFP features (68).

An alternative use for LFPs lies in identifying discrete states linked to movement. In electrocortical studies, a person's visual attention (versus eye movement) can be classified above chance levels into one of eight directions (69). In the posterior parietal cortex (PPC), 0–10- and 20–40-Hz bands revealed the onset of motion (70). This finding is an especially significant step because the decoding was done online when the monkey used an iBCI to perform the task. Thus, LFPs could

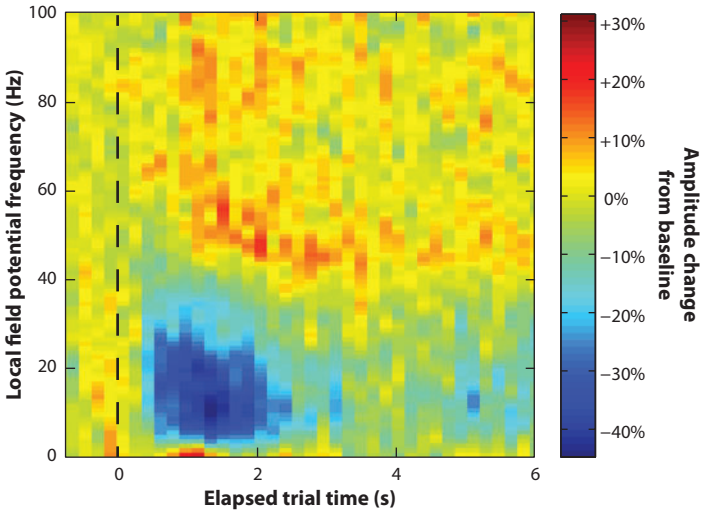

Figure 6

Representative spectrogram of the local field potential in one channel, averaged over 70 repeated trials. Time 0 denotes the instructed onset of movement (*dashed line*). Colors indicate amplitude, normalized by dividing by average baseline activity prior to movement onset (*blue* represents greatest reduction in activity; *red* represents greatest increase in activity). The data were recorded from a person with tetraplegia intending to move her own hand during repeated cursor control calibration trials. Note the appearance of at least three differing bands (approximately 0–3, 3–40, and 40–100 Hz). (Printed with permission from J.A. Perge, unpublished data.)

play a part in a hierarchal decoding strategy in which identification of the discrete motor state dictates how to approach estimating the continuous variables.

Also, the precise features extracted from these broadband neural signals can make a substantive difference in their decoding utility. Instead of LFP amplitude, recent work is starting to reveal the role of LFP phase. Investigations into beta oscillations, for example, have found a statistical dependence between the oscillation's phase and target reach direction (71). These observations are supported by the revealed coherence between beta oscillations and electromyography (EMG) recordings (72). Spiking activity has also been linked to the phase of beta oscillation, in that directional information of the former was a function of the latter (73). These new insights suggest that extracting phase information from LFPs might improve iBCI decoding by considering the influence of LFP waveform phase on modulations in spiking activity.

Decoder Calibration

Overview. In order to customize the decoder to a particular user, initial filter calibration exercises engage the iBCI user. In animals, the subject is trained to perform the behavioral task, using overt arm actions. Meanwhile, recordings of the brain activity are collected (16, 18–22). By contrast, people with paralysis are asked to attempt arm and hand motions that would, for example, generate planar mouse trajectories and clicks matching the computer controlled cursor on the screen (23, 74). In these calibration sessions, the recorded neural signals and any information processed from them are not presented to the user and thus are called open loop. Similar approaches can be used for initial calibration for the control of multidimensional reach and grasp movements of a robotic or prosthetic arm (25, 26).

The recorded neural signals and the corresponding movement information are then sent to calibration routines that set parameters within the decoder. For example, when a person with paralysis used an iBCI to control a computer cursor's motion, linear regression processed the calibration data to arrive at the needed matrices for the linear filter (23). In the case of a Bayesian classifier, once the neural signal samples are separated into their respective classes, class-conditioned distributions can be fit from the data, for example, calculating means for independent Poisson distributions (22). The calibration procedures usually extend to processing the features themselves. For instance, from the set of spiking units collected, only those modulating well with reach direction as shown through analysis of variance (ANOVA) were selected for inclusion in the decoder (21). Such steps help to best fit the decoder's parameters given the calibration data while protecting against over fitting.

Closed-loop calibration. The concept behind closed-loop calibration is to adjust the decoder's calibration after a closed-loop block of trials, where the iBCI is used to carry out the task. The process has an iterative nature such that the previous calibration block adjusts the decoder used in the next calibration block (19). Supporting the approach, differences were found in neuronal activity between actual and observed movement (75, 76). Furthermore, although observation-tuned neurons were found to be predictive of movement direction, strictly action-modulating neurons did a better job. Even more recently, such tuning differences, depending upon cognitive context, have also been reported in preliminary studies in clinical trial participants with tetraplegia (77).

Closed-loop decoder calibration has been used successfully to enable control in able-bodied monkeys (24, 78) and in people with tetraplegia (see **Figure 7**) (25, 26). An innovation is to run an automated software routine to assist epochs of neural control—that is, iBCI-controlled movements, as opposed to hand-controlled movements—thereby increasing trial success. In early iterations, considerable assistance is provided, but with each iteration it lessens until the task is completely governed by neural control. Not only is the technique thought to improve the decoder, but the user's neural activity appears to change to accommodate the iBCI. In several studies, the response characteristics of units changed as the monkey learned a task (79). When a tuned decoder was intentionally altered while a monkey was operating an iBCI, units' firing rates changed during continued use of the iBCI (33). In another closed-loop iBCI experiment, rats improved their

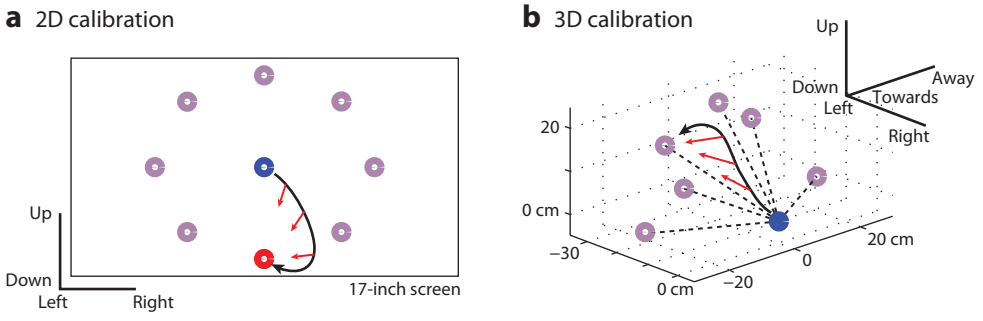

Figure 7

Illustration of the closed-loop calibration technique. (*a*) The black line shows cursor trajectory; the blue and red dots show the starting point and goal, respectively. At each sample time, the direction between the cursor and goal is calculated (*red arrows*). This direction is then compared with the current cursor heading in order to generate an error signal with which to adjust the decoding tuning parameters. (Printed with permission from B. Jarosiewicz, unpublished data.) (*b*) A similar technique can be applied in the 3D case. (Adapted with permission from Reference 25.)

task success rate without changing their overt behavior (80). Thus, use of closed-loop calibration appears to allow both the user and the decoder to update their internal calculations in an effort to converge on stable configurations for useful closed-loop iBCI operation.

Sometimes, long after a stable mapping has been achieved, it changes, making the initial decoding model inaccurate. Fortunately, there are mathematical frameworks to formalize possible paths of deviation and ways to fix this problem. On the efficiency side, a recursive least squares formulation can prevent one from having to reconsider all prior calibration blocks (81). Similarly, the problem can be cast in a Bayesian context (82). These innovations get closer to how best to utilize and efficiently process the closed-loop calibration data to adapt the decoder.

Dimensionality reduction and regularization. Several methods seek to remove or discount one or more neural activity feature(s) collected during filter calibration in order to make the decoding more accurate. One direct way to go about this is to focus on well-isolated single unit activity (SUA). By comparing changes in waveform characteristics, spike intervals, and directional tuning, one study chose a small subset of 10 to 15 units from the 75–100 that were recorded (32). The calibrated decoder performed well over many days (9 days in one monkey, 19 in another).

Others have employed more automated means, such as cross validation, whereby the calibration data are divided into three sets: training, validation, and assessment. First, the decoder training data are used to build models, that is, for the mathematical mapping between features and motor states. These models are then checked with the validation data set to see which performs best, and finally the true test of performance occurs with the assessment data. If models under comparison differ by the features chosen, then a greedy method, akin to forward stepwise regression, can find promising, though typically not optimal, subsets (83). This strategy has yielded reductions in the number of features chosen, in some cases by a factor of four, in 3D reach and grasp in monkeys (50, 58).

Alternatively, the decoder can treat the neural signal features as being driven by a small number of latent variables, which then represent motor intent—a technique called dimensionality reduction. Gaussian process factor analysis (GPFA), for example, both smooths in time and finds a smaller set of latent features (84). By using data from neural ensembles, GPFA was found to improve trajectory reconstruction accuracy over standard methods. Use of dimensionality reduction in real-time decoding reduced the number of variables driving the decoder by approximately 90% in one case and 60% in another (85). Furthermore, error rates in directional classification dropped dramatically from roughly 20% to 5%. Interestingly, such latent features may generate new theories about fundamental, computational principles of the motor cortex. In a reduced space, characteristic, repeatable oscillations emerged, suggesting that cell populations in motor cortex might not encode movement variables per se but rather serve as a pattern generator to drive downstream computations and eventually the movement itself (86).

These methods become particularly important if more advanced feature extraction methods are used. With LFP histories, the number of features can easily grow into the thousands. Given such a large data set, many of the features display a redundancy that can be taken advantage of to reject a variety of noise sources, such as those of a biological nature and recording artifacts. Dimensionality reduction and regularization are ways to contend with such disturbances and indeed have been successfully wielded to handle feature deluges of as many as 6,400 features in order to achieve stable performance in electrocorticography work over many days (87).

Motor State Estimation

Overview. Given a set of features extracted from the neural signals, computations estimate the intended motor state. Decoded motor states have focused largely on those surrounding arm

reaching and grasping, particularly as these functions are listed as most important to restore by people with high-cervical spinal cord injury (88). Specifically, many earlier studies investigated decoding end-point velocity and/or position in order to control the movement of a computer cursor on a screen (18–20, 23). For discrete selection, monkeys choose a reach target position/direction from a finite list of options (21, 22). One end goal of the work is to realize the possibility of enabling someone with loss of a limb or paralysis to control a robotic aid or FES-driven limb for reaching and grasping. The relatively high-level motor commands of selecting a target or controlling the end-point trajectory could then be converted to control commands needed to drive the effector.

A standard estimation approach is the linear filter (89), and it has been used for continuous decoding (e.g., 9, 18, 19, 23, 24). Each feature value specifies the length of a vector of fixed orientation in the motor state space. The vectors are then summed to yield the state estimate. For discrete states, Bayesian classifiers have also proven useful (21, 22). They typically model the feature distributions conditioned on the discrete states as either Poisson or Gaussian. Both methods have the advantage of being calibrated by exact methods, fast online computation times, and relative transparency in the behavior of the tuned estimator.

More accurate estimation models. However, in a head-to-head comparison between linear and Kalman filtering, the latter was shown to perform better, using several standard performance metrics of cursor control (90). Interestingly, as **Figure 8** shows, the Kalman filter did not always yield better cursor trajectories. The algorithm performs the estimation based upon linear, multivariate Gaussian models linking the features to the motor state as well as describing the motor state dynamics. The decoder can run on the same timescale as a linear filter because the results

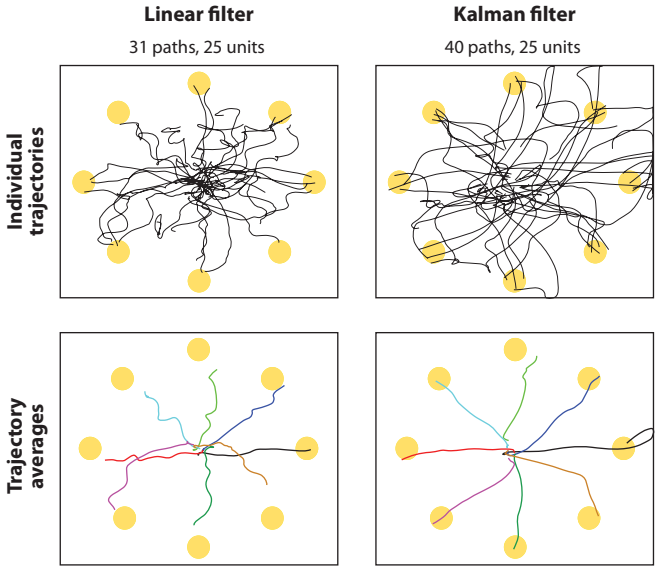

Figure 8

A comparison of the paths under brain control using the Kalman filter versus the linear filter. The paths were generated by a person with tetraplegia using velocity-based decoders during the eight-target, center-out task. Performance results are shown from two recording sessions in which both the linear filter and the Kalman filter were sequentially tested. The eight targets were located at 0°, 45°, 90°, 135°, 180°, 225°, 270°, and 315°. Units indicate the number of features employed by the respective decoding filter. (Reprinted with permission from Reference 90.)

from the linear algebra calculations quickly reach steady state (91). Of special note is the fact that the evaluation was done by people with tetraplegia operating an iBCI to control the motion of a computer cursor. Since then, the method has provided a reliable estimation approach, even in trials 1,000 days after implantation of the sensor (74). A variant of the technique recently enabled two people with severe paralysis to perform 3D reach and grasp tasks by way of a robotic arm aid (25), in one case more than five years after sensor implantation.

Careful evaluation of the true functional mapping showed a large fraction (35%) of the unit spike counts to be nonlinearly related to intended motor control states (92), and for this reason, some earlier attempts with iBCIs worked with nonlinear decoders (14). Another line of research added an autoregressive element to the feature histories (52, 93). By combining the two types of model refinements, animals were able to operate iBCIs within an unscented Kalman filter framework, yielding improved performance (94). Very general mappings between the features and states can be handled by particle filters (55, 95–97) or neural networks (14, 98).

Discrete motor states can also be introduced into the model. The resulting hybrid state-space model switches between a series of discrete modes (99). Computational machinery infers the state transitions during the model fitting process via methods such as expectation maximization (EM). The technique was applied to augment the Kalman filter (100) as well as a point process filter (101). The augmented set of hidden motor states, like the nonlinear models, frees the estimator from purely linear assumptions should the calibration data show a clear nonlinear relationship. In terms of metrics such as mean squared error, use of hybrid state models has achieved reductions as high as 22% (101). However, the results should be treated with caution, as the real test lies in closed-loop, head-to-head comparisons (102).

Improving the noise modeling, another line of inquiry makes the more accurate assumption that the spike counts follow a Poisson process (rather than a Gaussian distribution). This is the territory of point process models, and they account for the exact timing of the spiking sequences (99, 103). Unlike most linear filter methods, which process spike count features within, for example, 30-ms bins (24), point processes isolate each unit firing event in time for a typical time bin of 1 ms (104). In off-line studies, decoders running point process models have been demonstrated in animals (101, 105, 106) as well as with data collected from people with tetraplegia (104). The cost for the improved modeling fidelity, however, is that decoding becomes more computationally intensive.

Choice of motor control states. Increasing the degrees of freedom decoded from motor cortical activity would enable more tasks to be performed with an iBCI and/or tasks to be performed with a greater degree of control. Reports of 3D reach and grasp with a robotic arm in able-bodied monkeys (24) and in people with tetraplegia (25, 26) provide direct evidence of this and relied on expanding the state dimension from two to four (one extra spatial dimension and a variable for grasp). For more precise control, decoders could first determine whether or not the person was attempting a move and in what general direction. Initial creation of such a first-stage classifier was reported in monkeys (107). Even finer stages of motor preparation and execution can be detected with iBCIs; for example, pretrial, precue, memory (remembering target location during a delay), and post-saccade phases could be readily decoded in macaques (108).

Alternatively, the measured neural activity may be better associated with a different set of motor states. For example, a unit could be more tuned to wrist extension than to general upward motion (109). Responding to this need, researchers decoded 25 joint angles under natural reach and grasp conditions in monkeys (50) under open-loop conditions. The strategy relied on statistical dependencies between the joint angles, allowing the kinematic states to be compressed down to 10. As the 10 variables were estimated at each time step, a linear transform expanded the estimate to a vector representing all 25 joint angles. Thus, even with a relatively small sample of neurons

in motor cortex, iBCIs based on motor cortical recordings should enable complex reach and grasp movement. Forces are also encoded in the stream of neural activity measurements (8, 110). In planar manipulandum experiments, software simultaneously decoded force and velocity in off-line analyses (111). Estimating intended force (grip force, for example) in people with paralysis will be an important venture and is likely to benefit from feedback from the effector.

Decoding muscle contractions has led to monkeys regaining control of muscles in temporarily paralyzed limbs through FES driven by an iBCI. In 2008, monkeys were reported to control wrist torques in closed-loop experiments (27). More recently, five electrodes stimulated three muscles that drive wrist flexion and grip (29). Effectively building an artificial bridge from the central nervous system to the muscles, the animals were able to pick up balls and place them into a receptacle. For people, control of a virtual arm was shown possible by a person with tetraplegia, using a simulation that incorporates the complex, dynamic response behavior of an FES system (30). These advancements mark key milestones toward restoring limb control to those with paralysis.

Although the majority of studies in nonhuman primates have focused on reaching and grasping, research has also investigated other types of motor control. Going beyond hand grip, individual finger movements (i.e., which finger moved) have been correctly classified better than 80% of the time (112, 113) in off-line studies. Leg kinematic off-line decoding studies in monkeys have also been performed (114), although full closed-loop locomotion presents interlimb coordination and balance challenges. Rats, with electrodes in the hind-limb/trunk region of motor cortex, successfully lightened a load applied to their hips, in time with their gait (115). Although neither study demonstrated closed-loop control over the entire combination of movements needed to enable walking, they do suggest a route to the more modest goals of controlling walking direction and speed as well as making any major load adjustments.

Adaptive estimation. The relationship between the intended movement of a person with tetraplegia and the relatively tiny ensemble of neural signals used to deduce that intended movement is by no means expected to remain stationary. Although this relationship can be stable over time (32), both technical factors (e.g., micromotion of the electrode with respect to the tissue, changing characteristics of recording devices) and biological ones (e.g., cortical plasticity) discussed earlier can change the mapping (51, 116, 117). Thus, adaptive decoders have been employed to continually refine the relationship between the recorded neural signals and the expected output. For example, by using Bayesian regression methods, decoding performance was maintained in the face of model drift on the timescale of days (118).

Ultimately, the nonstationarities may arise from a range of cognitive or physiological state variables. For example, spikes rates may modulate by levels of attention. The amplitude of beta oscillations reduces upon initiation of movement (11), and the phasing of the rhythm has been shown to be predictive of spike activity (73). Thus, directly accounting for movement onset in the estimator may enable it to account for some of the nonstationarities. Similarly, incorporating eye position into the estimation process can raise iBCI performance (119). In this view, the observed nonstationarities reflect more the incomplete nature of existing models underlying estimators than changes to the random noise corrupting the neural signal.

SUMMARY

Research progress in implants and decoders for iBCIs is advancing rapidly. In 2006, people with paralysis had just begun to control a computer cursor and simple robotic devices. Only six years later, complex 3D reach and grasp movements using intracortically controlled assistive robotic devices was achieved (see **Figure 9**) (25, 26). Wireless, transcutaneous sensors have reached the

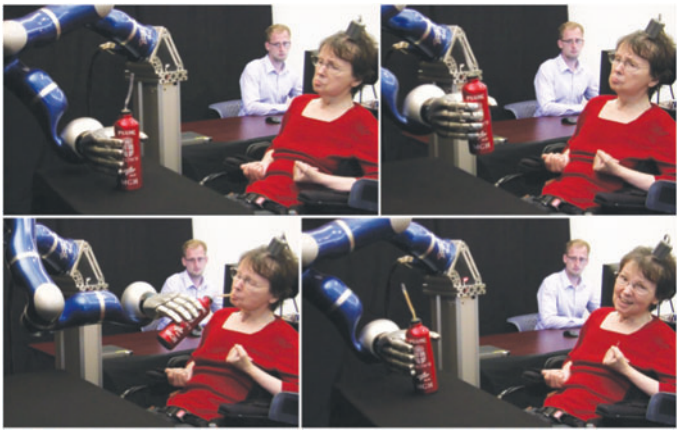

Figure 9

Successful iBCI-based neural control of a robotic arm, by a person with tetraplegia, to reach and grasp a thermos of coffee. The microelectrode array recording the neural data had been implanted for more than five years at the time of this achievement. (Reprinted with permission from Reference 25.)

milestone of initial successful animal testing (48). Furthermore, as has been the case in the neural prosthesis field for more than 50 years, publicly funded preclinical research continues to provide vital insights and new directions for clinical investigation focused on developing restorative neurotechnologies for people with paralysis.

At the same time, the number of decodable states is expanding (50), and other areas besides the arm are proving to be amenable to neural control (115). The push for additional motor states is supported by an expansion of the list of features extracted, such as those derived from LFPs (68, 87). These developments promise to increase the capability of robotic aids and prostheses.

Just as important as the degrees of freedom is the quality of control. With the introduction of algorithms such as dimensionality reduction (85) and improved implant circuitry, the neural signal features are becoming less contaminated by noise. Noise-free signals, however, will not cure errors in the model, but fortunately, model sophistication is increasing as well (90, 104), as are ways to avoid poor calibration (24, 25, 26). These efforts fuel hopes of seeing finer control tasks performed in the coming years.

Finally, for the technology to be clinically viable, it would ideally be reliable for very long time periods, with a span of more than a decade being a plausible target. Preliminary reports, with one person successfully using an investigational iBCI (BrainGate) for five years, suggest great potential; however, additional advances in sensor manufacturing will be essential (74). For example, the current work on a wireless, transcutaneous implant eliminates some connectors and tethering that can wear. When sensor characteristics change with time or the physiological mapping between intended movement and neural activity evolves, adaptive features built into the decoder can mitigate such deviations (118). These innovations all underscore the expectation that iBCI users will soon see implants functioning well for many years and iBCIs being used for days at a time without any recalibration.

The iBCI field is tasked simultaneously with creating better devices for fundamental neuroscience research and with creating viable clinical neurotechnologies. This latter goal requires continued advances in neuroengineering, as well as rigorous clinical evaluation. With iBCIs becoming more capable, precise, and reliable, future research will next need to bridge the gap between demonstrating a capability in a research context and incorporating the technology into

the daily lives of its users. For people who are unable to move or speak owing to brain stem stroke or motor neuron disease, the impact of even modest increases in command signal output will be immense. Although this and other goals for iBCIs will likely require years of additional research to become reality, recent strides make clear that such technologies are moving steadily from the realm of science fiction toward the domain of devices that support the communication, mobility, and independence of people with neurologic disease or injury.

DISCLOSURE STATEMENT

The authors are not aware of any affiliations, memberships, funding, or financial holdings that might be perceived as affecting the objectivity of this review.

ACKNOWLEDGMENTS

This work is supported in part by the Rehabilitation Research and Development Service, Office of Research and Development, US Department of Veterans Affairs. Additional support is provided by NIH [NIDCD (R01DC009899) and NIBIB (R01EB007401-01)], DARPA REPAIR (N66001-10-C-2010), Doris Duke Charitable Foundation, MGH-Deane Institute for Integrated Research on Atrial Fibrillation and Stroke, and the Katie Samson Foundation. The contents do not represent the views of the US Department of Veterans Affairs or the United States Government.

LITERATURE CITED

1. Ziegler-Graham K, MacKenzie EJ, Ephraim PL, Travison TG, Brookmeyer R. 2008. Estimating the prevalence of limb loss in the United States: 2005 to 2050. *Arch. Phys. Med. Rehabil.* 89:422–9
2. Christopher & Dana Reeve (CDR) Found. 2009. *One Degree of Separation: Paralysis and Spinal Cord Injury in the United States.* Short Hills, NJ: CDR Found.
3. Jackson AB, Dijkers M, Devivo MJ, Poczatek RB. 2004. A demographic profile of new traumatic spinal cord injuries: change and stability over 30 years. *Arch. Phys. Med. Rehabil.* 85:1740–48
4. Mak JN, Wolpaw JR. 2009. Clinical applications of brain-computer interfaces: current state and future prospects. *IEEE Rev. Biomed. Eng.* 2:187–99
5. Schalk G, Leuthardt EC. 2011. Brain-computer interfaces using electrocorticographic signals. *IEEE Rev. Biomed. Eng.* 4:140–54
6. Evarts EV. 1968. Relation of pyramidal tract activity to force exerted during voluntary movement. *J. Neurophysiol.* 31:14–27
7. Fetz EE. 1969. Operant conditioning of cortical unit activity. *Science* 163:955–58
8. Humphrey DR, Schmidt EM, Thompson WD. 1970. Predicting measures of motor performance from multiple cortical spike trains. *Science* 170:758–62
9. Georgopoulos AP, Schwartz AB, Kettner RE. 1986. Neuronal population coding of movement direction. *Science* 233:1416–19
10. Kalaska JF, Crammond DJ. 1992. Cerebral cortical mechanisms of reaching movements. *Science* 255:1517–23
11. Sanes JN, Donoghue JP. 1993. Oscillations in local field potentials of the primate motor cortex during voluntary movement. *Proc. Natl. Acad. Sci. USA* 90:4470–74
12. BeMent SL, Wise KD, Anderson DJ, Najafi K, Drake KL. 1986. Solid-state electrodes for multichannel multiplexed intracortical neuronal recording. *IEEE Trans. Biomed. Eng.* 33:230–41
13. Maynard EM, Nordhausen CT, Normann RA. 1997. The Utah Intracortical Electrode Array: a recording structure for potential brain-computer interfaces. *Electroencephalogr. Clin. Neurophysiol.* 102:228–39
14. Burrow M, Dugger J, Humphrey DR, Reed DJ, Hochberg LR. 1997. Cortical control of a robot using a time-delay neural network. *Proc. Int. Conf. Rehabil. Robot.* (*ICORR*), Bath, UK, April 14–18, pp. 83–86. Bath, UK: Bath Inst. Med. Eng.

15. Humphrey DR, Reed DJ, Hochberg LR, Burrow M, Dugger J. 1997. *Cortical control of neural prosthetic devices.* Final Rep. NIH/NINDS Contract N01-NS-1-2308. Bethesda, MD: Natl. Inst. Health/Natl. Inst. Neurol. Disord. Stroke
16. Chapin JK, Moxon KA, Markowitz RS, Nicolelis MA. 1999. Real-time control of a robot arm using simultaneously recorded neurons in the motor cortex. *Nat. Neurosci.* 2:664–70
17. Kennedy PR, Bakay RA. 1998. Restoration of neural output from a paralyzed patient by a direct brain connection. *Neuroreport* 9:1707–11
18. Serruya MD, Hatsopoulos NG, Paninski L, Fellows MR, Donoghue JP. 2002. Instant neural control of a movement signal. *Nature* 416:141–42
19. Taylor DM, Tillery SI, Schwartz AB. 2002. Direct cortical control of 3D neuroprosthetic devices. *Science* 296:1829–32
20. Carmena JM, Lebedev MA, Crist RE, O'Doherty JE, Santucci DM, et al. 2003. Learning to control a brain-machine interface for reaching and grasping by primates. *PLoS Biol.* 1:e42
21. Musallam S, Corneil BD, Greger B, Scherberger H, Andersen RA. 2004. Cognitive control signals for neural prosthetics. *Science* 305:258–62
22. Santhanam G, Ryu SI, Yu BM, Afshar A, Shenoy KV. 2006. A high-performance brain-computer interface. *Nature* 442:195–98
23. Hochberg LR, Serruya MD, Friehs GM, Mukand JA, Saleh M, et al. 2006. Neuronal ensemble control of prosthetic devices by a human with tetraplegia. *Nature* 442:164–71
24. Velliste M, Perel S, Spalding MC, Whitford AS, Schwartz AB. 2008. Cortical control of a prosthetic arm for self-feeding. *Nature* 453:1098–101
25. Hochberg LR, Bacher D , Jarosiewicz B, Masse NY, Simeral JD, et al. 2012. Reach and grasp by people with tetraplegia using a neurally controlled robotic arm. *Nature* 485:372–75
26. Collinger JL, Wodlinger B, Downey JE, Wang W, Tyler-Kabara EC, et al. 2013. High-performance neuroprosthetic control by an individual with tetraplegia. *Lancet* 381:557–64
27. Moritz CT, Perlmutter SI, Fetz EE. 2008. Direct control of paralysed muscles by cortical neurons. *Nature* 456:639–42
28. Pohlmeyer EA, Oby ER, Perreault EJ, Solla SA, Kilgore KL, et al. 2009. Toward the restoration of hand use to a paralyzed monkey: brain-controlled functional electrical stimulation of forearm muscles. *PLoS One* 4:e5924
29. Ethier C, Oby ER, Bauman MJ, Miller LE. 2012. Restoration of grasp following paralysis through brain-controlled stimulation of muscles. *Nature* 485:368–71
30. Chadwick EK, Blana D, Simeral JD, Lambrecht J, Kim SP, et al. 2011. Continuous neuronal ensemble control of simulated arm reaching by a human with tetraplegia. *J. Neural Eng.* 8:034003
31. Linderman MD, Santhanam G, Kemere CT, Gilja V, O'Driscoll S, et al. 2008. Signal processing challenges for neural prostheses. *IEEE Signal Proc. Mag.* 25:18–28
32. Ganguly K, Secundo L, Ranade G, Orsborn A, Chang EF, et al. 2009. Cortical representation of ipsilateral arm movements in monkey and man. *J. Neurosci.* 29:12948–56
33. Jarosiewicz B, Chase SM, Fraser GW, Velliste M, Kass RE, Schwartz AB. 2008. Functional network reorganization during learning in a brain-computer interface paradigm. *Proc. Natl. Acad. Sci. USA* 105:19486–91
34. Wolpaw JR, Wolpaw EW. 2012. *Brain-Computer Interfaces: Principles and Practice*. Oxford, UK: Oxford Univ. Press
35. Robinson DA. 1968. Electrical properties of metal microelectrodes. *Proc. Inst. Electrical Electron. Eng.* 56:1065–71
36. Jones KE, Campbell PK, Normann RA. 1992. A glass silicon composite intracortical electrode array. *Ann. Biomed. Eng.* 20:423–37
37. Bai Q, Wise KD. 2001. Single-unit neural recording with active microelectrode arrays. *IEEE Trans. Biomed. Eng.* 48:911–20
38. Kipke DR, Vetter RJ, Williams JC, Hetke JF. 2003. Silicon-substrate intracortical microelectrode arrays for long-term recording of neuronal spike activity in cerebral cortex. *IEEE Trans. Neural Syst. Rehabil. Eng.* 11:151–55

39. Yousry TA, Schmid UD, Alkadhi H, Schmidt D, Peraud A, et al. 1997. Localization of the motor hand area to a knob on the precentral gyrus. A new landmark. *Brain* 120:141–57
40. Bhandari R, Negi S, Rieth L, Normann RA, Solzbacher F. 2009. A novel masking method for high aspect ratio penetrating microelectrode arrays. *J. Micromech. Microeng.* 19:035004
41. Seymour JP, Langhals NB, Anderson DJ, Kipke DR. 2011. Novel multi-sided, microelectrode arrays for implantable neural applications. *Biomed. Microdevices* 13:441–51
42. Abidian MR, Ludwig KA, Marzullo TC, Martin DC, Kipke DR. 2009. Interfacing conducting polymer nanotubes with the central nervous system: chronic neural recording using poly(3,4-ethylenedioxythiophene) nanotubes. *Adv. Mater.* 21:3764–70
43. Ludwig KA, Langhals NB, Joseph MD, Richardson-Burns SM, Hendricks JL, Kipke DR. 2011. Poly(3,4-ethylenedioxythiophene) (PEDOT) polymer coatings facilitate smaller neural recording electrodes. *J. Neural Eng.* 8:014001
44. Santhanam G, Linderman MD, Gilja V, Afshar A, Ryu SI, et al. 2007. HermesB: a continuous neural recording system for freely behaving primates. *IEEE Trans. Biomed. Eng.* 54:2037–50
45. Chestek CA, Gilja V, Nuyujukian P, Kier RJ, Solzbacher F, et al. 2009. HermesC: low-power wireless neural recording system for freely moving primates. *IEEE Trans. Neural Syst. Rehabil. Eng.* 17:330–38
46. Harrison RR, Kier RJ, Chestek CA, Gilja V, Nuyujukian P, et al. 2009. Wireless neural recording with single low-power integrated circuit. *IEEE Trans. Neural Syst. Rehabil. Eng.* 17:322–29
47. Miranda H, Gilja V, Chestek C, Shenoy KV, Meng TH. 2009. A high-rate long-range wireless transmission system for multichannel neural recording applications. *IEEE Int. Symp. Circuits Syst.* (*ISCAS*), May 24–27, pp. 1265–68. Piscataway, NJ: IEEE
48. Yin M, Borton DA, Aceros J, Patterson WR, Nurmikko AV. 2012. A 100-channel hermetically sealed implantable device for wireless neurosensing applications. *IEEE Int. Symp. Circuits Syst.* (*ISCAS*), May 20–23, pp. 2629–32. Piscataway, NJ: IEEE
49. Borton DA, Yin M, Aceros J, Nurmikko AV. 2013. An implantable wireless neural interface for recording cortical circuit dynamics in moving primates. *J. Neural Eng.* 10:026010
50. Vargas-Irwin CE, Shakhnarovich G, Yadollahpour P, Mislow JM, Black MJ, Donoghue JP. 2010. Decoding complete reach and grasp actions from local primary motor cortex populations. *J. Neurosci.* 30:9659–69
51. Kim SP, Wood F, Fellows M, Donoghue JP, Black MJ. 2006. Statistical analysis of the non-stationarity of neural population codes. *IEEE/RAS-EMBS Int. Conf. Biomed. Robot. Biomechatron.*, 1st, Pisa, Italy, Feb. 20–22, pp. 811–816. Piscataway, NJ: IEEE
52. Shpigelman L, Lalazar H, Vaadia E. 2009. Kernel-ARMA for hand tracking and brain-machine interfacing during 3D motor control. *Adv. Neural Inf. Proc. Syst.* 21:1489–96
53. Chestek CA, Gilja V, Nuyujukian P, Foster JD, Fan JM, et al. 2011. Long-term stability of neural prosthetic control signals from silicon cortical arrays in rhesus macaque motor cortex. *J. Neural Eng.* 8:045005
54. Perge JA, Homer ML, Malik WQ, Friehs G, Donoghue JP, Hochberg LR. 2013. Intra-day signal instabilities affect decoding performance in an intracortical neural interface system. *J. Neural Eng.* 10:036004
55. Fraser GW, Chase SM, Whitford A, Schwartz AB. 2009. Control of a brain-computer interface without spike sorting. *J. Neural Eng.* 6:055004
56. Humphrey DR. 2001. Systems, methods, and devices for controlling external devices by signals derived directly from the nervous system. *US Patent No. 6,171,239*
57. Stark E, Abeles M. 2007. Predicting movement from multiunit activity. *J. Neurosci.* 27:8387–94
58. Zhuang J, Truccolo W, Vargas-Irwin C, Donoghue JP. 2010. Decoding 3-D reach and grasp kinematics from high-frequency local field potentials in primate primary motor cortex. *IEEE Trans. Biomed. Eng.* 57:1774–84
59. Malik WQ, Stavisky SD, Bacher D, Simeral JD, Truccolo W, et al. 2010. Decoding multiunit activity in neural interfaces for individuals with tetraplegia. *Neurosci. Meet. Plan.*, program no. 899.3. San Diego, CA: Soc. Neurosci.
60. Buzsaki G, Anastassiou CA, Koch C. 2012. The origin of extracellular fields and currents—EEG, ECoG, LFP and spikes. *Nat. Rev. Neurosci.* 13:407–20

61. Bouyer JJ, Montaron MF, Rougeul A. 1981. Fast fronto-parietal rhythms during combined focused attentive behaviour and immobility in cat: cortical and thalamic localizations. *Electroencephalogr. Clin. Neurophysiol.* 51:244–52
62. Mehring C, Rickert J, Vaadia E, Cardosa de Oliveira S, Aertsen A, Rotter S. 2003. Inference of hand movements from local field potentials in monkey motor cortex. *Nat. Neurosci.* 6:1253–54
63. Rickert J, Oliveira SC, Vaadia E, Aertsen A, Rotter S, Mehring C. 2005. Encoding of movement direction in different frequency ranges of motor cortical local field potentials. *J. Neurosci.* 25:8815–24
64. Scherberger H, Jarvis MR, Andersen RA. 2005. Cortical local field potential encodes movement intentions in the posterior parietal cortex. *Neuron* 46:347–54
65. Bansal AK, Truccolo W, Vargas-Irwin CE, Donoghue JP. 2012. Decoding 3D reach and grasp from hybrid signals in motor and premotor cortices: spikes, multiunit activity, and local field potentials. *J. Neurophysiol.* 107:1337–55
66. Ince NF, Gupta R, Arica S, Tewfik AH, Ashe J, Pellizzer G. 2010. High accuracy decoding of movement target direction in non-human primates based on common spatial patterns of local field potentials. *PLoS One* 5:e14384
67. Bansal AK, Vargas-Irwin CE, Truccolo W, Donoghue JP. 2011. Relationships among low-frequency local field potentials, spiking activity, and three-dimensional reach and grasp kinematics in primary motor and ventral premotor cortices. *J. Neurophysiol.* 105:1603–19
68. Flint RD, Lindberg EW, Jordan LR, Miller LE, Slutzky MW. 2012. Accurate decoding of reaching movements from field potentials in the absence of spikes. *J. Neural Eng.* 9:046006
69. Gunduz A, Brunner P, Daitch A, Leuthardt EC, Ritaccio AL, et al. 2012. Decoding covert spatial attention using electrocorticographic (ECoG) signals in humans. *Neuroimage* 60:2285–93
70. Hwang EJ, Andersen RA. 2009. Brain control of movement execution onset using local field potentials in posterior parietal cortex. *J. Neurosci.* 29:14363–70
71. Rubino D, Robbins KA, Hatsopoulos NG. 2006. Propagating waves mediate information transfer in the motor cortex. *Nat. Neurosci.* 9:1549–57
72. Baker SN. 2007. Oscillatory interactions between sensorimotor cortex and the periphery. *Curr. Opin. Neurobiol.* 17:649–55
73. Reimer J, Hatsopoulos NG. 2010. Periodicity and evoked responses in motor cortex. *J. Neurosci.* 30:11506–15
74. Simeral JD, Kim SP, Black MJ, Donoghue JP, Hochberg LR. 2011. Neural control of cursor trajectory and click by a human with tetraplegia 1000 days after implant of an intracortical microelectrode array. *J. Neural Eng.* 8:025027
75. Tkach D, Reimer J, Hatsopoulos NG. 2008. Observation-based learning for brain-machine interfaces. *Curr. Opin. Neurobiol.* 18:589–94
76. Dushanova J, Donoghue J. 2010. Neurons in primary motor cortex engaged during action observation. *Eur. J. Neurosci.* 31:386–98
77. Feldman JM, King B, Truccolo W, Hochberg LR, Donoghue JD. 2011. Decoding neural representations of action from motor cortex ensembles during action observation in humans with tetraplegia. *Neurosci. Meet Plan.*, program no. 142.14. Washington, DC: Soc. Neurosci.
78. Orsborn AL, Dangi S, Moorman HG, Carmena JM. 2012. Closed-loop decoder adaptation on intermediate time-scales facilitates rapid BMI performance improvements independent of decoder initialization conditions. *IEEE Trans. Neural Syst. Rehabil. Eng.* 20:468–77
79. Green AM, Kalaska JF. 2011. Learning to move machines with the mind. *Trends Neurosci.* 34:61–75
80. Koralek AC, Jin X, Long JD II, Costa RM, Carmena JM. 2012. Corticostriatal plasticity is necessary for learning intentional neuroprosthetic skills. *Nature* 483:331–35
81. Wu W, Hatsopoulos NG. 2008. Real-time decoding of nonstationary neural activity in motor cortex. *IEEE Trans. Neural Syst. Rehabil. Eng.* 16:213–22
82. Li Z, O'Doherty JE, Lebedev MA, Nicolelis MA. 2011. Adaptive decoding for brain-machine interfaces through Bayesian parameter updates. *Neural Comput.* 23:3162–204
83. Hastie T, Tibshirani R, Friedman J. 2009. *The Elements of Statistical Learning: Data Mining, Inference, and Prediction*. New York: Springer. 2nd ed.

84. Yu BM, Cunningham JP, Santhanam G, Ryu SI, Shenoy KV, Sahani M. 2009. Gaussian-process factor analysis for low-dimensional single-trial analysis of neural population activity. *J. Neurophysiol.* 102:614–35
85. Santhanam G, Yu BM, Gilja V, Ryu SI, Afshar A, et al. 2009. Factor-analysis methods for higher-performance neural prostheses. *J. Neurophysiol.* 102:1315–30
86. Churchland MM, Cunningham JP, Kaufman MT, Foster JD, Nuyujukian P, et al. 2012. Neural population dynamics during reaching. *Nature* 487:51–56
87. Chao ZC, Nagasaka Y, Fujii N. 2010. Long-term asynchronous decoding of arm motion using electrocorticographic signals in monkeys. *Front. Neuroeng.* 3:3
88. Anderson KD. 2004. Targeting recovery: priorities of the spinal cord-injured population. *J. Neurotrauma* 21:1371–83
89. Oppenheim AV, Schafer RW. 2010. *Discrete-Time Signal Processing*. Upper Saddle River, NJ: Prentice Hall. 3rd ed.
90. Kim SP, Simeral JD, Hochberg LR, Donoghue JP, Black MJ. 2008. Neural control of computer cursor velocity by decoding motor cortical spiking activity in humans with tetraplegia. *J. Neural Eng.* 5:455–76
91. Malik WQ, Truccolo W, Brown EN, Hochberg LR. 2011. Efficient decoding with steady-state Kalman filter in neural interface systems. *IEEE Trans. Neural Syst. Rehabil. Eng.* 19:25–34
92. Paninski L, Shoham S, Fellows MR, Hatsopoulos NG, Donoghue JP. 2004. Superlinear population encoding of dynamic hand trajectory in primary motor cortex. *J. Neurosci.* 24:8551–61
93. Fisher J, Black M. 2005. Motor cortical decoding using an autoregressive moving average model. *Conf. Proc. IEEE Eng. Med. Biol. Soc.* 2:2130–33
94. Li Z, O'Doherty JE, Hanson TL, Lebedev MA, Henriquez CS, Nicolelis MA. 2009. Unscented Kalman filter for brain-machine interfaces. *PLoS One* 4:e6243
95. Gao Y, Black M, Bienenstock E, Shoham S, Donoghue J. 2002. Probabilistic inference of hand motion from neural activity in motor cortex. *Adv. Neural Inf. Proc. Syst.* 1:213–20
96. Brockwell AE, Rojas AL, Kass RE. 2004. Recursive Bayesian decoding of motor cortical signals by particle filtering. *J. Neurophysiol.* 91:1899–907
97. Wood F, Prabhat, Donoghue J, Black M. 2005. Inferring attentional state and kinematics from motor cortical firing rates. *Conf. Proc. IEEE Eng. Med. Biol. Soc.* 1:149–52
98. Sussillo D, Nuyujukian P, Fan JM, Kao JC, Stavisky SD, et al. 2012. A recurrent neural network for closed-loop intracortical brain-machine interface decoders. *J. Neural Eng.* 9:026027
99. Srinivasan L, Eden UT, Mitter SK, Brown EN. 2007. General-purpose filter design for neural prosthetic devices. *J. Neurophysiol.* 98:2456–75
100. Wu W, Black MJ, Mumford D, Gao Y, Bienenstock E, Donoghue JP. 2003. A switching Kalman filter model for the motor cortical coding of hand motion. *Conf. Proc. IEEE Eng. Med. Biol. Soc.* 3:2083–86
101. Lawhern V, Wu W, Hatsopoulos N, Paninski L. 2010. Population decoding of motor cortical activity using a generalized linear model with hidden states. *J. Neurosci. Methods* 189:267–80
102. Chase SM, Schwartz AB, Kass RE. 2009. Bias, optimal linear estimation, and the differences between open-loop simulation and closed-loop performance of spiking-based brain-computer interface algorithms. *Neural Netw.* 22:1203–13
103. Brown EN, Frank LM, Tang D, Quirk MC, Wilson MA. 1998. A statistical paradigm for neural spike train decoding applied to position prediction from ensemble firing patterns of rat hippocampal place cells. *J. Neurosci.* 18:7411–25
104. Truccolo W, Friehs GM, Donoghue JP, Hochberg LR. 2008. Primary motor cortex tuning to intended movement kinematics in humans with tetraplegia. *J. Neurosci.* 28:1163–78
105. Truccolo W, Eden UT, Fellows MR, Donoghue JP, Brown EN. 2005. A point process framework for relating neural spiking activity to spiking history, neural ensemble, and extrinsic covariate effects. *J. Neurophysiol.* 93:1074–89
106. Nazarpour K, Ethier C, Paninski L, Rebesco JM, Miall RC, Miller LE. 2012. EMG prediction from motor cortical recordings via a nonnegative point-process filter. *IEEE Trans. Biomed. Eng.* 59:1829–38
107. Kemere C, Santhanam G, Yu BM, Afshar A, Ryu SI, et al. 2008. Detecting neural-state transitions using hidden Markov models for motor cortical prostheses. *J. Neurophysiol.* 100:2441–52
108. Campos M, Breznen B, Andersen RA. 2010. A neural representation of sequential states within an instructed task. *J. Neurophysiol.* 104:2831–49

109. Kakei S, Hoffman DS, Strick PL. 2003. Sensorimotor transformations in cortical motor areas. *Neurosci. Res.* 46:1–10
110. Fagg AH, Ojakangas GW, Miller LE, Hatsopoulos NG. 2009. Kinetic trajectory decoding using motor cortical ensembles. *IEEE Trans. Neural Syst. Rehabil. Eng.* 17:487–96
111. Gupta R, Ashe J. 2009. Offline decoding of end-point forces using neural ensembles: application to a brain-machine interface. *IEEE Trans. Neural Syst. Rehabil. Eng.* 17:254–62
112. Acharya S, Tenore F, Aggarwal V, Etienne-Cummings R, Schieber MH, Thakor NV. 2008. Decoding individuated finger movements using volume-constrained neuronal ensembles in the M1 hand area. *IEEE Trans. Neural Syst. Rehabil. Eng.* 16:15–23
113. Baker J, Bishop W, Kellis S, Levy T, House P, Greger B. 2009. Multi-scale recordings for neuroprosthetic control of finger movements. *Conf. Proc. IEEE Eng. Med. Biol. Soc.* 2009:4573–77
114. Fitzsimmons NA, Lebedev MA, Peikon ID, Nicolelis MA. 2009. Extracting kinematic parameters for monkey bipedal walking from cortical neuronal ensemble activity. *Front. Integr. Neurosci.* 3:3
115. Song W, Giszter SF. 2011. Adaptation to a cortex-controlled robot attached at the pelvis and engaged during locomotion in rats. *J. Neurosci.* 31:3110–28
116. Perge JA, Donoghue JP, Hochberg LR. 2010. Firing rate nonstationarity can contribute to performance variations in neural cursor control: a BrainGate2 study. *Neurosci. Meet. Plan.*, program no. 899.10. San Diego, CA: Soc. Neurosci.
117. Gilja V, Chestek CA, Diester I, Henderson JM, Deisseroth K, Shenoy KV. 2011. Challenges and opportunities for next-generation intracortically based neural prostheses. *IEEE Trans. Biomed. Eng.* 58:1891–99
118. Li Z, O'Doherty E, Lebedev MA, Nicolelis MA. 2010. Closed-loop adaptive decoding using Bayesian regression self-tuning. *Neurosci. Meet. Plan.*, program no. 383.10. San Diego, CA: Soc. Neurosci.
119. Batista AP, Yu BM, Santhanam G, Ryu SI, Afshar A, Shenoy KV. 2008. Cortical neural prosthesis performance improves when eye position is monitored. *IEEE Trans. Neural Syst. Rehabil. Eng.* 16:24–31

Annual Review of Biomedical Engineering
Volume 15, 2013

Contents

Indexes

Errata

An online log of corrections to *Annual Review of Biomedical Engineering* articles may be found at http://bioeng.annualreviews.org/